



OPEN ACCESS

EDITED BY

Senhu Lin,
Research Institute of Petroleum
Exploration and Development (RIPE),
China

REVIEWED BY

Pengyuan Zhang,
Chinese Academy of Sciences (CAS),
China
Tao Hu,
China University of Petroleum, China

*CORRESPONDENCE

Enze Wang,
✉ wangenze9939@163.com

RECEIVED 07 October 2023

ACCEPTED 31 October 2023

PUBLISHED 28 December 2023

CITATION

Wang E, Guo T, Dong X and Wang T
(2023), Pore system and methane
adsorption capacity features of marine
and marine-continental transitional shale
in the Sichuan Basin, SW China.
Front. Earth Sci. 11:1308815.
doi: 10.3389/feart.2023.1308815

COPYRIGHT

© 2023 Wang, Guo, Dong and Wang. This
is an open-access article distributed
under the terms of the [Creative
Commons Attribution License \(CC BY\)](#).
The use, distribution or reproduction in
other forums is permitted, provided the
original author(s) and the copyright
owner(s) are credited and that the original
publication in this journal is cited, in
accordance with accepted academic
practice. No use, distribution or
reproduction is permitted which does not
comply with these terms.

Pore system and methane adsorption capacity features of marine and marine-continental transitional shale in the Sichuan Basin, SW China

Enze Wang^{1,2*}, Tonglou Guo³, Xiaoxia Dong⁴ and Tong Wang⁴

¹State Key Laboratory of Shale Oil and Gas Enrichment Mechanisms and Effective Development, Beijing, China, ²School of Earth and Space Sciences, Peking University, Beijing, China, ³Southwest Oil & Gas Company, SINOPEC, Chengdu, Sichuan, China, ⁴Research Institute of Exploration and Development, SINOPEC Southwest Oil and Gas Company, Chengdu, Sichuan, China

Recently, significant achievements have been made in the gas exploration of marine Longmaxi shale in China. As exploration efforts have advanced, the exploration targets have gradually expanded to other sedimentary systems (marine-continental transitional and lacustrine). Compared with marine shale, shale in other sedimentary systems shows stronger heterogeneity, rendering previous exploration experiences of marine shale ineffective in guiding exploration efforts. Therefore, there is a pressing need for comparative studies to support future exploration practices. In this paper, the marine Longmaxi Formation and the marine-continental transitional Longtan Formation shales in the Lintanchang area of the southeastern of the Sichuan Basin are selected as the research objects. The study aims to compare the mineralogical characteristics, pore systems, and methane adsorption capacities of these two sets of shales, thereby revealing the differences in controlling factors that affect their physical properties and methane adsorption capacities. Our results show that the Longtan shale exhibits a higher clay mineral content, while the Longmaxi shale demonstrates significantly higher siliceous mineral content. Compare with Longmaxi shale, the Longtan shale exhibits a wider distribution range and higher average value of TOC content. The pore system in the Longmaxi shale is primarily dominated by organic matter-related pores, whereas the Longtan shale is characterized by clay mineral-related pores as the primary pore type. Given the variance in sedimentary environments, the controlling factors of physical properties differ significantly between the two sets of shales. In the case of the Longmaxi shale, TOC content is the most influential factor governing physical properties, while clay mineral content exerts the most significant influence on physical properties in the Longtan shale. Furthermore, TOC content emerges as the primary factor affecting methane adsorption capacity in both the Longmaxi and Longtan shales, despite the presence of significant variations in their pore systems. Nevertheless, the specific mechanisms through which TOC content impacts methane adsorption capacity exhibit variations between the two distinct shale types under investigation. The difference in sedimentary environment leads to various

effects of mineral composition on methane adsorption capacity. Therefore, in the future research, the influences of different factors on methane adsorption capacity should be studied in combination with the sedimentary background.

KEYWORDS

shale gas, marine shale, marine-continental transitional shale, pore system, methane adsorption capacity

1 Introduction

In recent years, unconventional oil and gas have emerged as the primary focus of the petroleum industry, with shale gas being commercially developed in several countries (Ross and Bustin, 2008; Zou et al., 2016; Wang et al., 2020; Wu et al., 2021; Li et al., 2021; Wang et al., 2022a; Wang et al., 2022b; Hu et al., 2022; Li et al., 2022; Zhou et al., 2022; Feng et al., 2023; Jin, 2023; Yang et al., 2023; Zhou et al., 2023). The United States, for instance, has achieved significant shale gas production, reaching $7330 \times 10^8 \text{ m}^3$ (Zou et al., 2021). Substantial advancements have also been made in the exploration and development of the marine Longmaxi shale in the Sichuan Basin, China (Dong et al., 2018; Wang et al., 2022b; Yin et al., 2022). The exploration practices have unveiled the remarkable resource potential of shale gas, consequently attracting widespread attention from both academia and industry. As development progresses, shale of other sedimentary systems (marine-continental transitional and lacustrine) has become the focus of exploration (Wang et al., 2022; Wang et al., 2023). Marine-continental transitional shale is a new field of shale gas exploration recently (Zou et al., 2016; Wang et al., 2022c). Exploration practices have already demonstrated promising prospects in the Permian Longtan Formation within the Sichuan Basin and the Permian Shanxi Formation within the Ordos Basin (Dong et al., 2021). Previous study indicates that the shale gas resource potential of marine-continental transitional shale in China can reach $19.8 \times 10^{12} \text{ m}^3$ (Yin et al., 2021; Lu et al., 2023), highlighting the substantial reserves that have spurred academic research in this field (Wu et al., 2021; Dong et al., 2021; Qiu et al., 2021). However, strong heterogeneity has rendered previous exploration experiences in marine shale inadequate for effectively guiding exploration efforts. Consequently, there is an urgent need for more comparative studies to support and inform future exploration practices.

There are three occurrence status of gas in shale: free state, adsorption state, and dissolved state (Curtis, 2002; Ross and Bustin, 2008; Zhou et al., 2018). Adsorption gas is mainly adsorbed on organic matter (OM) and clay mineral particles. Previous studies have shown that adsorbed gas accounts for up to 60% of total gas content (GIP, Curtis, 2002; Zhou et al., 2018; Chen et al., 2021; Shi et al., 2022). Therefore, accurately characterizing the methane adsorption capacity of shale holds significant importance. The methane adsorption capacity of shale is controlled by many geological factors, including OM content, kerogen type, mineral composition, pore structure characteristics, etc. (Sander et al., 2018; He et al., 2019; Gao et al., 2020; Shi et al., 2022; Wang et al., 2023; Xin et al., 2023). While current research on the methane adsorption capacity of marine shale has yielded relatively clear findings, the main controlling factors for methane adsorption capacity in marine-continental transitional facies remain insufficiently understood.

Meanwhile, compared with marine shale, the complexity and the proportions of the various type of pores of marine-continental transitional shale exhibit obvious differences (Wang et al., 2022c). It is evident that these distinct differences in pore systems (types, physical properties, and pore size) will have non-negligible effects on methane adsorption capacity (Xu et al., 2019).

The Sichuan Basin is renowned for being one of the most abundant petroliferous basins in China, particularly in terms of natural gas resources (Liu et al., 2020). Within this basin, the Permian Longtan Formation shale has emerged as a significant target for marine-continental transitional shale gas exploration in China (Dong et al., 2021; Wang et al., 2022c). This paper focuses on systematically characterizing the mineralogical features, pore system, and methane adsorption capacity of two sets of shales: the marine Longmaxi shale and the marine-continental transitional Longtan shale. To accomplish this, drilling samples from the Lintanchang area in the southeastern part of the Sichuan Basin were carefully selected. Through a comparative analysis of the geological characteristics of these two sets of shales, as well as an exploration of the main controlling factors affecting their physical properties and methane adsorption capacity, this study aims to provide a theoretical foundation for the exploration of marine-continental transitional shale gas in the Sichuan Basin.

2 Geological setting

The Sichuan Basin is one of the main petroliferous basins in China, with an area of $18 \times 10^4 \text{ km}^2$, the resource potential of natural gas is approximately $21.7 \times 10^{12} \text{ m}^3$ (Wang et al., 2022c; Zhang et al., 2022; Zhang et al., 2023). Within the Sichuan Basin, three distinct shale petroleum systems can be identified, characterized by different sedimentary environments. These systems are arranged from bottom to top as follows: the marine system comprising the Ediacaran Doushantuo Formation, Cambrian Qiongzhusi Formation, and Ordovician-Silurian Wufeng-Longmaxi Formation; the marine-continental transitional system including the Permian Qixia-Maokou Formation and Longtan-Changxing Formation; and the lacustrine system consisting of the Triassic Xujiahe Formation and Jurassic Ziliujing-Liangaoshan Formation.

The Longmaxi Formation shale in the Sichuan Basin is mainly formed in an anoxic deep-shallow shelf sedimentary environment with large differences in depth, ranging from 2,000 to 7,000 m (Feng et al., 2023). The lithology of the Longmaxi shale primarily consists of siltstone, gray shale, and black shale interbedded with siltstone. In terms of thermal maturity, the Longmaxi shale in the Sichuan Basin has generally reached the high-mature to over-mature stage, with an

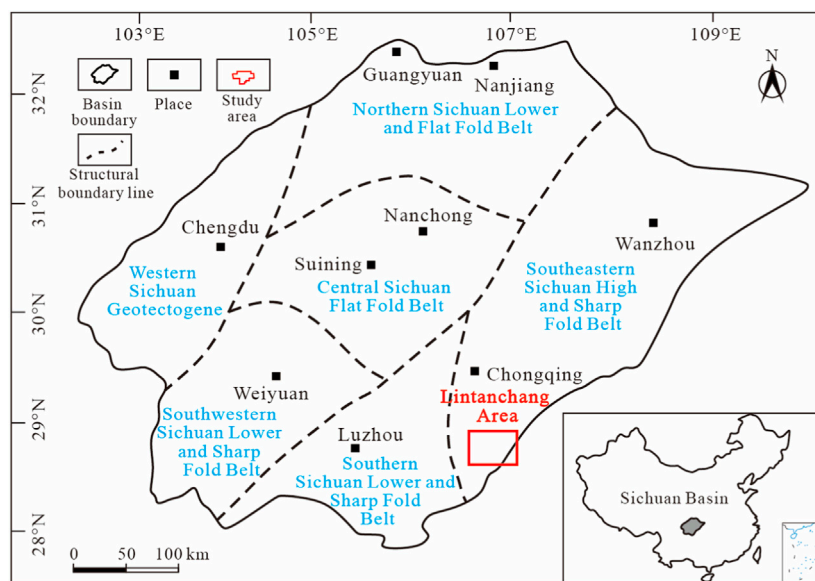


FIGURE 1
Geological figure of the Sichuan Basin and Location of the Lintanchang Area (modified by Wang et al., 2022b).

equivalent vitrinite reflectance ranging from about 2.0% to 3.6% (Dai et al., 2014). The Longtan shale in Sichuan Basin primarily associated with swamp and lagoon environments. Its lithology is predominantly composed of black-gray shale interbedded with thin coal layers (Dong et al., 2021). Similar to the Longmaxi shale, the Longtan shale also generally exhibits high-mature to over-mature thermal maturity (Wang et al., 2022c). The study area is located in the Lintanchang area in the southeastern of Sichuan Basin (Figure 1). In this area, the depth of the Longmaxi shale in the borehole typically exceeds 4,000 m, ranging from approximately 4,060–4,130 m, while the depth range of the Longtan shale spans from 3,160 to 3,240 m.

3 Data and method

3.1 Samples

The samples in this paper are all collected from the Longmaxi shale and the Longtan shale of LY3 well in Lintanchang area. The dataset comprises a total of 46 samples, with 18 samples obtained from the Longmaxi Formation and 28 samples from the Longtan Formation. The study incorporates various experiments and tests to investigate the shale properties, including total organic carbon (TOC) content, X-ray diffraction (XRD) test, helium porosity test, field emission scanning electron microscopy (FE-SEM) observation, N₂ adsorption test, and methane isothermal adsorption test. Part of the data (such as SEM observation, TOC content and N₂ adsorption test) are referred from references Wang et al. (2022b) and Wang et al. (2022c). The isothermal adsorption experiments were carried out at the Experimental Research Center of East China Branch, China Petroleum and Chemical Corporation (SINOPEC).

3.2 Experiments and langmuir model

Except the isothermal adsorption experiment, details of other tests can be found in the references Wang et al. (2022b) and Wang et al. (2022c). In order to characterize the methane adsorption capacity of the selected 46 samples, a series of steps were followed. Firstly, the samples were crushed to a particle size of 40–80 meshes. Subsequently, the crushed samples were loaded into an Isothermal Adsorption Analyzer (IsoSORP-HP Statical), and high-purity methane (99.9%) was employed as the adsorbate. The experiment encompassed 14 pressure points, with a maximum pressure of 30 MPa. To replicate the adsorption behavior under geological conditions, different experimental temperatures were employed for the Longmaxi and Longtan shales. Specifically, a temperature of 115°C was utilized for the Longmaxi shale, while a temperature of 90°C was used for the Longtan shale. It should be emphasized that the measured data represents the excess adsorption capacity of the shale samples. In this study, the Langmuir model, which is based on monolayer adsorption, was employed to analyze and interpret the methane adsorption characteristics. The formula is shown in Eq. 1.

$$V_{ex} = V_L \times P / (P_L + P) \times (1 - \rho_g / \rho_a) \quad (1)$$

Where the V_{ex} is excess adsorption capacity m³/t; V_L is the Langmuir volume, m³/t; P_L is the Langmuir pressure, MPa; P is the experiment pressure, MPa; ρ_g is the gas phase density of methane, g/cm³; ρ_a is the density of methane adsorption phase, g/cm³.

4 Result

4.1 Mineral composition and TOC content

The TOC content and mineral composition of the Longmaxi and Longtan shales in the study area are shown in Table 1 and

TABLE 1 TOC content and mineral composition of Longmaxi and Longtan shales.

Formation	TOC (%)	Quartz (%)	Feldspar (%)	Carbonate (%)	Dolomite (%)	Siderite (%)	Clay mineral (%)
Longmaxi	0.65-6.43 (2.00)	21-67 (32)	3-16 (9)	4-16 (8)	Trace amount-6 (2)	Trace amount	11-59 (46.0)
Longtan	0.10-10.39 (2.35)	6-39 (18.5)	Trace amount-7 (trace amount)	Trace amount-51 (4.4)	Trace amount-49 (10.8)	Trace amount-70 (12.4)	14-79 (49.3)

Note: minimum-maximum (average value).

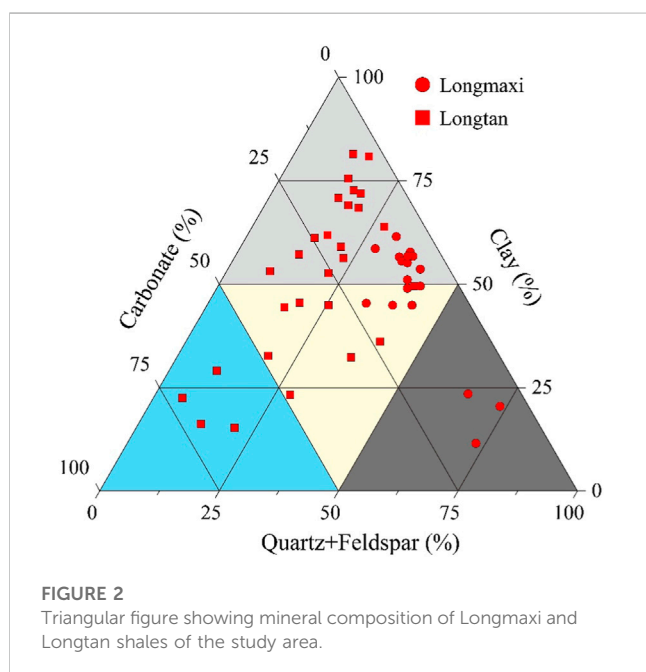


Figure 2. It can be observed that clay minerals are the predominant mineral types in both sets of shale. In the Longmaxi shale, the distribution range of clay minerals is 11%–59%, with an average content of 46.0%. The Longtan shale exhibits a slightly higher clay mineral content, with a range of 14%–79% and an average content of 49.3%. The primary difference in mineral composition between the Longmaxi Formation and Longtan Formation shales is in the content of siliceous and carbonate minerals. The Longmaxi shale shows a wider range of siliceous minerals, varying from 28% to 72% (average value of 41%), while the Longtan shale has a narrower range of 6%–39% (average value of 19%). Similarly, the distributions of carbonate minerals in the two sets of shale differ, with the Longmaxi shale ranging from 6% to 21% (average value of 10%), and the Longtan shale ranging from 3% to 70% (average value of 27%). Quartz is the predominant siliceous mineral, while feldspar content is relatively low. Calcite is the primary carbonate mineral in the Longmaxi shale, whereas the Longtan shale is characterized by the presence of dolomite and siderite as the main types of carbonate minerals. The OM content of the Longmaxi shale and Longtan shale are 0.65%–6.43% (average value 2.00%) and 0.10%–10.39% (average value 2.35%), respectively. The Longtan shale exhibits a higher average TOC content and a broader range of values compared to the Longmaxi shale.

4.2 Characteristics of pore system

4.2.1 Pore type

The pore system of the shale is known to be complex (Loucks et al., 2009), in order to systematically classify the pores of Longmaxi and Longtan shales, we select the classification of proposed by Chen et al. (2019). According to the relationship between pores and minerals (OM), the shale pores are divided into three categories, namely, organic matter-related pores (OMP), clay mineral-related pores (CMP), and framework mineral-related pores (FMP). For accurately identify the pore types, the FE-SEM observation is used to characterize the pore types of Longmaxi Formation and Longtan Formation shale in the study area. The geometry features of pores are shown in Figure 3.

Various pores show different development features in the shales. OMP is well developed in Longmaxi shale, these pores typically exhibit irregular shapes with good connectivity and small pore diameters, primarily in the nanoscale range (Figures 3A, B). While in the Longtan shale, nanosized OMPs are not widely observed in the OM grains. Instead, the main form of OMPs in the Longtan shale is represented by shrinkage fractures at the edges of OM grain. The pore sizes of these OMPs, ranging from nanoscale to microscale, are generally larger than those observed in the Longmaxi shale (Figures 3C, D). The CMPs can be detected both in Longmaxi and Longtan shales, which mainly occur as shrinkage fractures and intercrystalline pores within the clay minerals (Figures 3E–H). The pore size of CMPs are generally nanosized with medium connectivity. In the Longmaxi shale, CMPs are primarily developed in the illite-smectite mixed layer, while in the Longtan shale, CMPs are predominantly observed in the illite-smectite mixed layer and chlorite. Compared to the Longmaxi shale, the proportion of CMPs is relatively higher in the Longtan shale. FMP is mainly nano to micro-sized pores formed by the dissolution of framework grains (Figures 3I–M), and show irregular feature. Typically, these pores are isolated within framework grains. In the Longmaxi shale, the main dissolution minerals are calcite and feldspar, while in the Longtan shale, primary dolomite and siderite contribute to the dissolution minerals. Overall, the proportion of FMPs in the pore system of both shales is not high. In summary, the Longmaxi shale exhibits better development of OMPs compared to the Longtan shale, while the pore system of the Longtan shale is primarily dominated by CMPs. Although the dissolution minerals differ between the two shale formations, the proportion of FMPs in the pore system is not significant in either case.

4.2.2 Physical properties and N₂ adsorption

The physical properties of the Longmaxi and Longtan shales in the study area are shown in Table 2. The porosity ranges of the

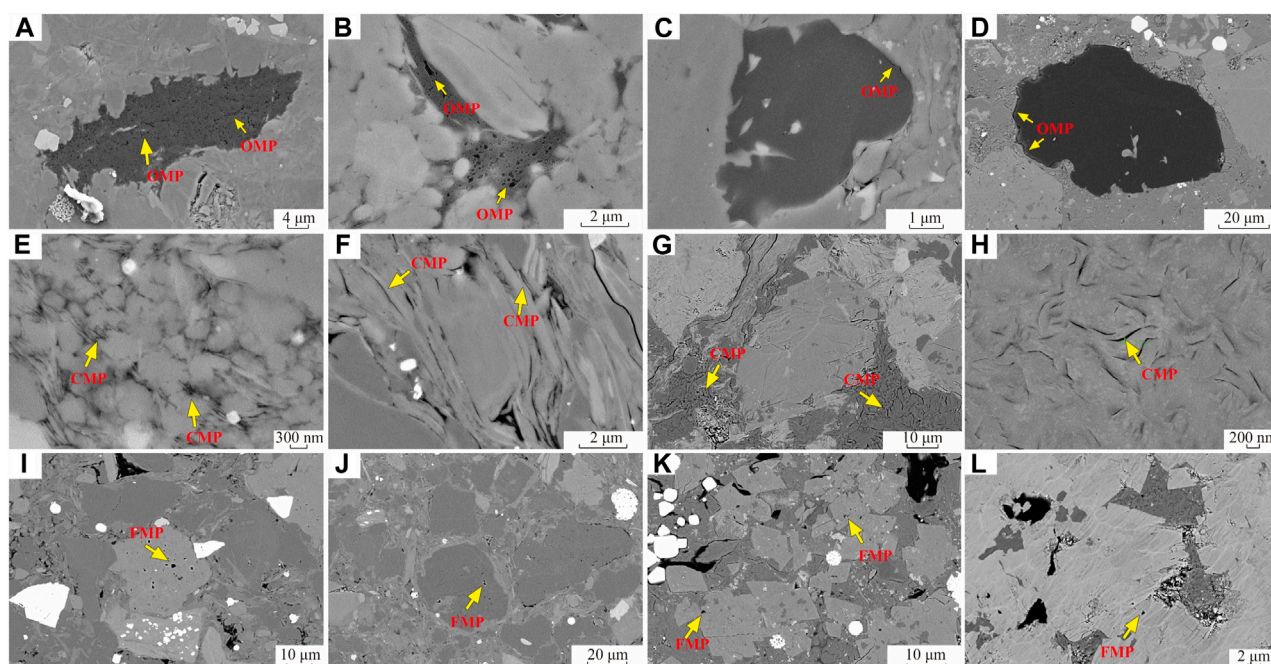


FIGURE 3

Pore system of Longmaxi and Longtan shales observed by FE-SEM. (A). Longmaxi Formation, 4081.72 m, large amount nano-sized organic matter-related pores; (B). Longmaxi Formation, 4130.70 m, well-developed nano-sized organic matter-related pores; (C). Longtan Formation, 3185.04 m, shrinkage features on the edge of organic matter; (D). Longtan Formation, 3156.41 m, shrinkage features on the edge of organic matter; (E). Longmaxi Formation, 4129.44 m, clay mineral-related intercrystalline pores; (F). Longmaxi Formation, 4117.88 m, clay mineral-related intercrystalline pores; (G). Longtan Formation, 3185.04 m, well-developed clay mineral-related intercrystalline pores; (H). Longtan Formation, 3173.48 m, well-developed clay mineral-related intercrystalline pores; (I). Longmaxi Formation, 4108.04 m, dissolution framework grains-related pores, the dissolution mineral is calcite; (J). Longmaxi Formation, 4095.45 m, dissolution framework grains-related pores, the dissolution mineral is feldspar; (K). Longtan Formation, 3161.23 m, dissolution framework grains-related pores, the dissolution mineral is dolomite; (L). Longtan Formation, 3208.26 m, dissolution framework grains-related pores, the dissolution mineral is siderite.

Longmaxi and Longtan shales are 0.52%–9.04% (average value 3.40%) and 1.66%–8.17% (average value 3.96%). The physical properties of Longtan shale are slightly higher than those of Longmaxi shale.

In order to quantitatively characterize the pore structure parameters of shale, N_2 adsorption test was used in this study. The typical N_2 adsorption curves of the two sets of shale are shown in Figure 4. In terms of curve shape, there is almost no significant difference between Longmaxi and Longtan shales in the study area. Both curves exhibit an anti-S shape and belong to type IV according to the classification of the International Union of Pure and Applied Chemistry (IUPAC, Thommes et al., 2015). The adsorption capacity shows a gradual increase at low relative pressures (less than 0.8) and then increases significantly beyond a certain threshold (more than 0.8). Obvious hysteresis loops can be observed in curves, indicating the presence of mesopores (2–50 nm) in shales. According to the IUPAC classification, the hysteresis loop of N_2 adsorption in the Longmaxi and Longtan Formation shales belongs to the mixed type of H2 and H3, indicating that the pores in the shale are ink bottle-and slit-shaped pores. It should be noted that the N_2 adsorption capacities of different shale are various. The N_2 adsorption capacity of Longmaxi shale ranges from 8.94 to 23.90 cm^3/g (average value is 13.99 cm^3/g), and N_2 adsorption capacity of Longtan shale varies from 2.83 to 27.44 cm^3/g (average value is 15.37 cm^3/g).

The pore volume (PV), specific surface area (SSA), and pore size distribution of shale are quantitatively characterized by N_2 adsorption. The pore structure parameters are shown in Table 2. The results show that the PV of the Longmaxi shale ranges from 0.0085 to 0.0222 cm^3/g (average value is 0.0136 cm^3/g), and the SSA of the Longmaxi shale varies from 3.49 to 22.08 m^2/g (average value is 12.27 m^2/g); while the range of PV and SSA of Longtan shale are 0.0037–0.0325 cm^3/g (average value is 0.0183 cm^3/g) and 0.77–18.82 m^2/g (average value is 6.82 m^2/g), respectively. Both shales exhibit a similar dominant pore size distribution, which is primarily composed of mesopores with a pore diameter of 3–5 nm (Wang et al., 2022b; Wang et al., 2022c). The contribution of pores with different pore sizes to pore structure parameters is shown in Table 2. It is observed that mesopores have the most significant control effect on both PV and SSA in both the Longmaxi and Longtan shales. Mesopores contribute dominantly to the SSA, with a contribution rate generally greater than 80%. However, the contribution rate of macropores to PV cannot be ignored, with an average contribution rate of 34.2% for the two sets of shales.

4.3 Methane isothermal adsorption features

The isothermal adsorption curves of Longmaxi and Longtan shales in the study area are shown in Figure 5. The adsorption capacity initially increases and then decreases as the pressure

TABLE 2 Physical properties and methane adsorption capacity of Longmaxi and Longtan shales.

Formation	Porosity (%)	V_L (m^3/t)	P_L (Mpa)	PV (cm^3/g)			SSA (m^2/g)				
				Total	Micropore	Mesopore	Macropore	Total	Micropore	Mesopore	Macropore
Longmaxi	0.52-9.04 (3.40)	1.38-3.85 (2.44)	3.66-9.61 (7.17)	0.0085-0.0222 (0.0136)	0.0002-0.0005 (0.0003)	0.0056-0.0169 (0.0092)	0.0027-0.0070 (0.0041)	3.5-22.1 (12.3)	0.24-1.45 (0.89)	2.8-20.8 (11.1)	0.2-1.1 (0.3)
Longtan	1.66-8.71 (3.96)	0.33-7.08 (2.40)	3.27-9.79 (5.29)	0.0037-0.0325 (0.0183)	0.00003-0.0004 (0.0002)	0.0019-0.0230 (0.0118)	0.0017-0.0112 (0.0063)	0.8-18.8 (6.8)	0.01-0.89 (0.44)	0.7-18.2 (6.1)	0.1-0.7 (0.3)

Minimum-maximum (average value).

increases, reaching a maximum value at approximately 10 MPa. This trend can be attributed to the increased gas phase density with higher experimental pressures. Meanwhile, it should be noted that there are two types of isothermal adsorption curves in both sets of shales under high pressure. The first type of curve exhibits no significant downward trend, as seen in samples like the 4132.34 m sample of Longmaxi shale and the 3171.97 m sample of Longtan shale. In contrast, the second type of curve shows a notable decrease in adsorption capacity as the pressure increases, such as the 4065.85 m sample of Longmaxi shale and the 3195.42 m sample of Longtan shale. This discrepancy is attributed to variations in the adsorbed phase density of the samples, reflecting the difference in the pore structure of samples (Shi et al., 2022). In this paper, V_L is used as a parameter to evaluate the methane adsorption capacity of shale. The V_L of Longmaxi and Longtan shales is shown in Table 2. The V_L distribution ranges of the Longmaxi and Longtan shales are 1.38–3.85 m^3/t (average value is 2.44 m^3/t) and 0.33–7.08 m^3/t (average value is 2.40 m^3/t), respectively. The V_L values indicate that the Longtan shale exhibits stronger heterogeneity in terms of methane adsorption capacity compared to the Longmaxi shale.

5 Discussion

5.1 Controlling factors of shale physical properties

The main controlling factors of physical properties of Longtan and Longmaxi shales in the study area are obviously different (Figure 6). The positive correlation between porosity, pore structure parameters, and TOC content (Figures 6A–C) in the Longmaxi shale suggests that OMP play a significant role in determining the pore system. This finding aligns with the results obtained from FE-SEM observation, where well-developed OMPs were observed (Wang et al., 2022b). However, the correlation between TOC content and physical properties in Longtan shale is notably weaker. The weak positive correlation with PV suggests a limited contribution of OMPs in the pore system of Longtan shale. This disparity in OMP development between the two shales may be attributed to differences in kerogen type. Previous studies have indicated that Longmaxi shale predominantly consists of type II kerogen, whereas Longtan shale contains a substantial amount of terrigenous higher plants, primarily type III kerogen (Dong et al., 2018; Wang et al., 2022c). Type III kerogen inherited from terrigenous higher plants may not generate abundant nanosized OMPs but instead exhibit shrinkage fractures at the edge of OM grains (Figures 3A–D; Yang et al., 2016). Although these edge shrinkage fractures have larger pore sizes, they are relatively less numerous compared to the nanosized OMPs observed in Longmaxi shale. Consequently, the varying pore system characteristics between the two shales lead to differing effects of TOC content on their physical properties.

The clay minerals content in shale reservoirs can have both positive and negative effects on their physical properties (Loucks et al., 2009; Furmann et al., 2014; Wang et al., 2022b). First, clay minerals contribute to the formation of CMP, which are an

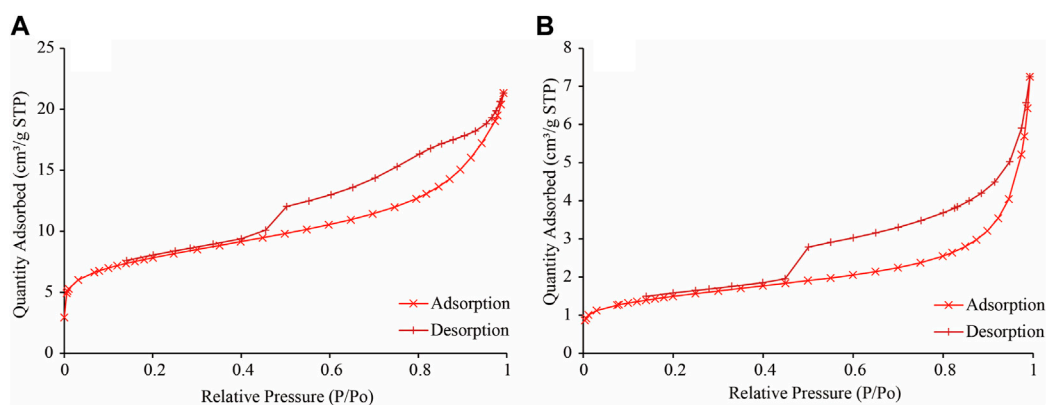


FIGURE 4 Typical N₂ adsorption curves of Longmaxi and Longtan shales. (A). Longmaxi Formation, 4132.34 m, TOC=5.16%; (B). Longtan Formation, 3,159.32 m, TOC=1.35%.

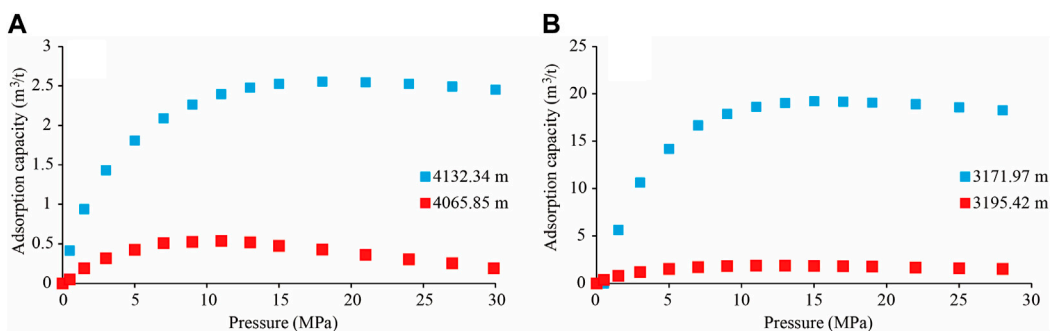
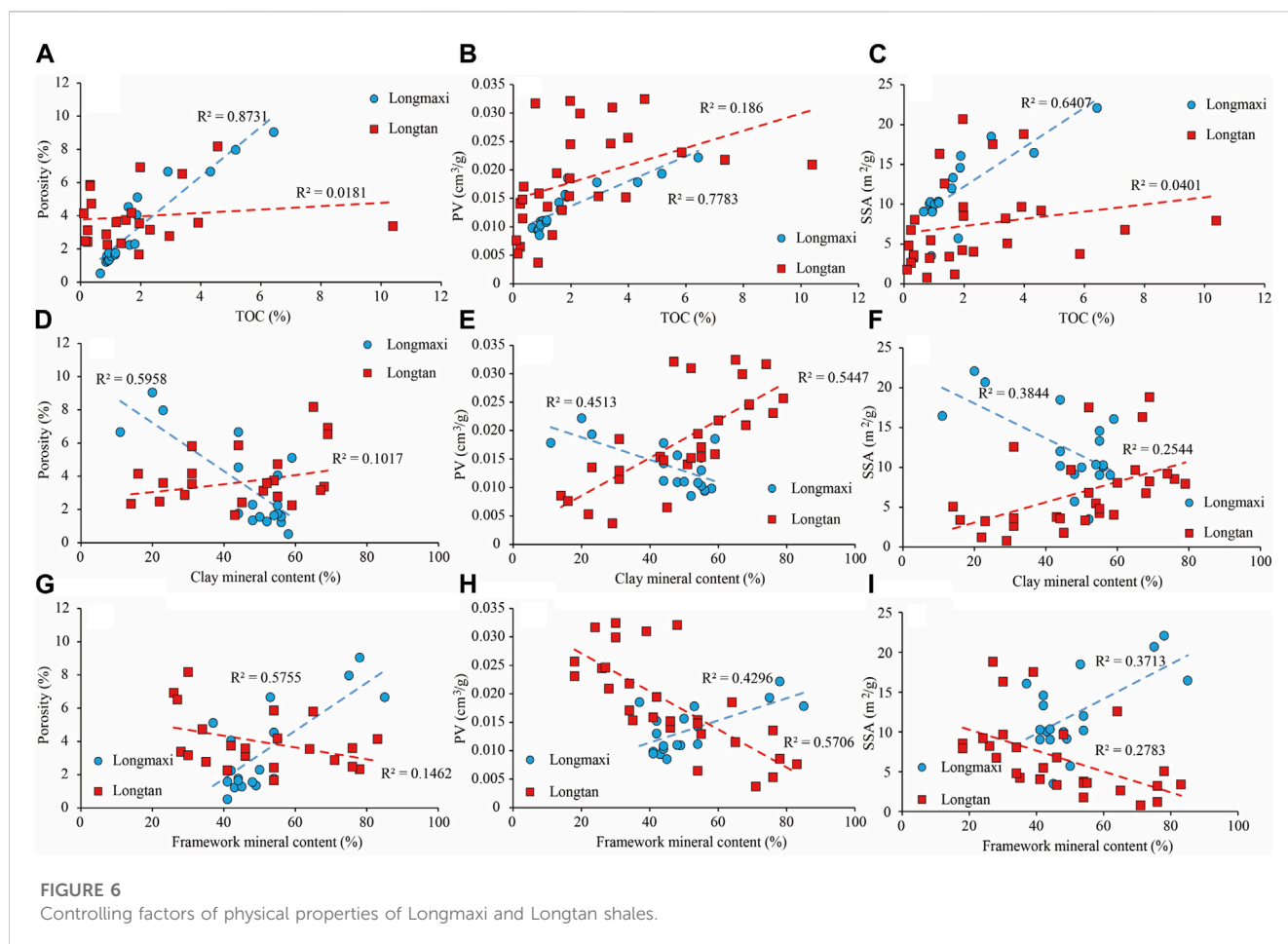


FIGURE 5 Typical methane isothermal adsorption curves of Longmaxi and Longtan shales. (A). Longmaxi Formation; (B). Longtan Formation.

important component of the pore system (Figures 3E–H). However, a high clay mineral content can also reduce the compaction resistance ability of shale, leading to the destruction of pores formed through diagenesis and OM thermal evolution (OMP, dissolution FMP, etc.). The effect of clay mineral content on physical properties is complex and varies between the two sets of shale studied. In the case of the Longmaxi shale, an increase in clay mineral content significantly reduces its physical properties. There are two main reasons for this phenomenon. Firstly, the increase in clay mineral content weakens the compaction resistance ability of the shale. Secondly, the OM enrichment of Longmaxi shale is mainly controlled by redox conditions and primary productivity (Wang et al., 2022b; Feng et al., 2023). High clay mineral content often indicates a high influx of terrigenous debris, which disrupts the original anoxic environment in the water column. This disruption leads to a decrease in TOC content and a reduction in the material basis for the development of OMP. Therefore, in the case of the Longmaxi shale, clay mineral content has a significant negative impact on its physical properties. In the case of Longtan shale, CMP dominates the pore system, and OMP has a limited effect on physical properties. Additionally, the enrichment of OM in Longtan shale mainly depends on terrigenous nutrients and OM input. In this

context, high clay mineral content is conducive to the formation of OMP (Wang et al., 2022c).

In contrast to the clay mineral content, a high framework mineral content represents the strong compaction resistance capacity of shale (Wang et al., 2022b), which contributes to the preservation of pores. However, the influence of framework mineral content on the physical properties of the two sets of shale differs significantly. In the case of the Longmaxi shale, the presence of siliceous content represents primary productivity, such as biogenic silica (Wang et al., 2022b; Feng et al., 2023). Consequently, the framework mineral content not only promotes the development of FMP, but also to the OM enrichment and the formation of OMP. For the Longtan shale, although an increase in framework mineral content can enhance the compaction resistance capacity and contribute to FMP formation, CMP play a more significant role in the pore system, and the contribution of FMP to the physical properties is considerably lower compared to that of CMP. Additionally, as the framework mineral content increases, there is a corresponding decrease in clay mineral content, which is unfavorable for CMP formation. As a result, a significant negative correlation exists between framework mineral content and physical properties in the Longtan shale.



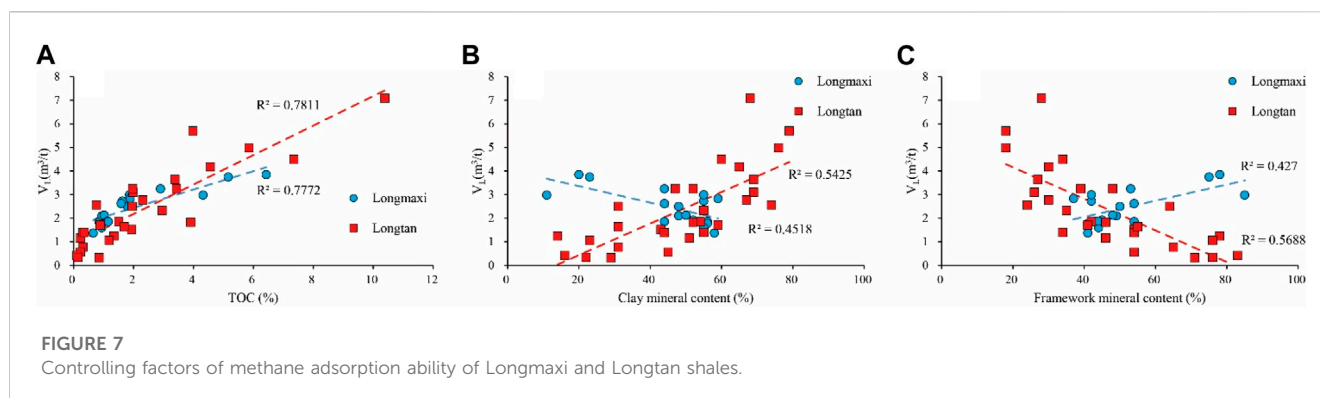
It should be emphasized that, as shown in Figure 6, the correlations between the physical properties and TOC content and mineral composition of the Longtan Formation are relatively poor. This reflects that the pore system of Longtan Formation shale is more complex, and various types of pores together constitute the pore system. Therefore, high determination coefficients (R^2) cannot be obtained by single factor analysis. In summary, the variation in sedimentary environment and OM enrichment mechanisms results in diverse pore types in the two sets of shale, consequently leading to different factors influencing their physical properties.

5.2 Influence factors of methane adsorption ability

In order to reveal the influencing factors of methane adsorption ability, the correlation analysis of V_L is shown in Figure 7. The results demonstrate a significant positive correlation between V_L and TOC content for two sets of shale. Notably, the R^2 of the Longtan shale is slightly higher than that of Longmaxi shale (Figure 7A). This shows that OM plays a vital role in methane adsorption. Although the two sets of shale exhibit similar trends, their underlying mechanisms differ significantly. In the case of Longmaxi shale, the dominant presence of OMP leads to a substantial positive correlation between TOC content and physical properties. Therefore, besides the methane adsorption

capacity associated with OM, the abundance of OMP provides additional space for methane adsorption. However, for the Longtan shale, there is no significant correlation between TOC content and physical properties. Hence, the influence of TOC content on V_L primarily reflects the methane adsorption capacity of OM. In this context, the higher R^2 value for Longtan shale suggests that different kerogen types exhibit varying methane adsorption capacities. To further quantify this difference, the parameter V_L/TOC is utilized to evaluate the methane adsorption capacity per unit TOC content. The results indicate that the V_L/TOC values of Longmaxi shale ranges from 0.6 to 2.2 $\text{m}^3/(\text{t}\cdot\%)$, with an average value of 1.6 $\text{m}^3/(\text{t}\cdot\%)$; the V_L/TOC of Longtan shale varies from 0.4 to 5.0 $\text{m}^3/(\text{t}\cdot\%)$, with an average value of 1.7 $\text{m}^3/(\text{t}\cdot\%)$. These findings highlight that type III kerogen demonstrates significantly higher methane adsorption capacity compared to type II kerogen, consistent with previous research (Lamberson and Bustin, 1993; Shi et al., 2022).

In addition to TOC content, mineral composition also exerts a significant control on V_L . Generally, clay minerals are known to have a strong adsorption capacity for methane (Tang and Fan, 2014), while siliceous and carbonate minerals exhibit relatively weak adsorption capacities. As a result, one would expect a positive correlation between clay mineral content and methane adsorption capacity, while the framework mineral content should have little effect. However, in this study, both clay mineral content and framework mineral content show a significant effect on V_L . The



clay mineral content has the opposite control effect on V_L . The high clay mineral content in the Longmaxi shale, indicative of increased terrigenous debris influx, leads to a decrease in TOC content and OMP development. In contrast, in the Longtan shale, where CMP dominates the pore system, high clay mineral content promotes primary productivity. Consequently, the methane adsorption capacity is improved in the Longtan shale through both increased OM content and an improved pore system. Similarly, the opposite effect of framework mineral content on V_L in the two shales is attributed to the differential influence of framework mineral content on TOC content and the pore system. Overall, while there are notable differences in pore systems, TOC content remains the most crucial factor controlling methane adsorption capacity. Furthermore, the varying sedimentary environments give rise to the differential effects of mineral composition on the methane adsorption capacity of shale. Therefore, future research should consider studying the effects of different factors on methane adsorption capacity in conjunction with the sedimentary background to gain a comprehensive understanding.

6 Conclusion

- 1) The Longtan shale exhibits a higher clay mineral content compared to the Longmaxi shale, while the Longmaxi shale has significantly higher siliceous mineral content than the Longtan shale. The TOC content of the Longtan shale displays a wider distribution range and a higher average value.
- 2) Three types of pores are identified in the shales, namely: OMP, CMP, and FMP. The Longmaxi shale is predominantly characterized by nanosized OMP, whereas the OMP in the Longtan shale primarily consists of shrinkage fractures at the edges of OM edge. CMP development is significantly more pronounced in the Longtan shale compared to the Longmaxi shale, and CMP represents the main pore type in the Longtan shale. FMP in the two sets of shale is mainly attributed to dissolution pores, and the proportion of FMPs in the pore system is not significant in either case.
- 3) In the case of the Longmaxi shale, TOC content is the most influential factor governing physical properties, and the presence of framework minerals also has a positive impact. The increase of clay mineral content is not conducive to the formation of high-quality reservoirs. Conversely, in the Longtan shale, clay mineral content plays a crucial role in controlling physical properties.

- 4) While notable disparities exist in the pore systems, it is evident that TOC content remains the most important factor influencing methane adsorption capacity. Nevertheless, the specific mechanisms through which TOC content impacts methane adsorption capacity exhibit variations between the two distinct shale types under investigation. In the case of the Longtan shale, the correlation between TOC content and methane adsorption capacity primarily stems from the methane adsorption capacity associated with OM. While the Longmaxi shale presents a compelling scenario wherein a substantial quantity of OMP development significantly contributes to the robust correlation observed between TOC content and methane adsorption capacity. The variations in mineral composition result in opposing effects on methane adsorption capacity. It is imperative to acknowledge that the effects of identical factors on methane adsorption capacity may vary in different sedimentary environments. Therefore, future research should investigate the impact of different factors on methane adsorption capacity in conjunction with the sedimentary background.

Data availability statement

The original contributions presented in the study are included in the article/Supplementary material, further inquiries can be directed to the corresponding author.

Author contributions

EW: Conceptualization, Data curation, Writing—original draft. TG: Supervision, Writing—review and editing. XD: Data curation, Writing—review and editing. TW: Data curation, Writing—review and editing.

Funding

The author(s) declare financial support was received for the research, authorship, and/or publication of this article. This study is supported by the open fund of State Key Laboratory of Shale oil and Gas Enrichment Mechanisms and Effective Development (Project No. 33550000-22-ZC0613-0337).

Conflict of interest

Authors TG, XD, and TW are employed by the SINOPEC Southwest Oil and Gas Company.

The remaining author declares that the research was conducted in the absence of any commercial or financial relationships that could be construed as a potential conflict of interest.

References

- Chen, L., Jiang, Z. X., Liu, Q. X., Jiang, S., Liu, K. Y., Tan, J. Q., et al. (2019). Mechanism of shale gas occurrence: insights from comparative study on pore structures of marine and lacustrine shales. *Mar. Pet. Geol.* 104, 200–216. doi:10.1016/j.marpetgeo.2019.03.027
- Chen, J. B., Zhang, C., Li, X. Y., Zhang, Y. K., and Wang, X. Q. (2021). Simulation of methane adsorption in diverse organic pores in shale reservoirs with multi-period geological evolution. *Int. J. Coal Sci. Technol.* 8 (5), 844–855. doi:10.1007/s40789-021-00431-7
- Curtis, J. B. (2002). Fractured shale-gas systems. *AAPG Bull.* 86 (11), 1921–1938. doi:10.1306/61eeddb-173e-11d7-8645000102c1865d
- Dai, J., Zou, C., Liao, S., Dong, D., Ni, Y., Huang, J., et al. (2014). Geochemistry of the extremely high thermal maturity Longmaxi shale gas, southern Sichuan Basin. *Org. Geochem.* 74, 3–12. doi:10.1016/j.orggeochem.2014.01.018
- Dong, D. Z., Qiu, Z., Zhang, L. F., Li, S. X., Zhang, Q., Li, X. T., et al. (2021). Progress on sedimentology of transitional facies shales and new discoveries of shale gas. *Acta Sedimentol. Sin.* 39 (1), 29–45. doi:10.14027/j.issn.1000-0550.2021.002
- Dong, D. Z., Shi, Z. S., Guan, Q. Z., Jiang, S., Zhang, M. Q., Zhang, C. C., et al. (2018). Progress, challenges and prospects of shale gas exploration in the Wufeng–Longmaxi reservoirs in the Sichuan Basin. *Nat. Gas. Ind.* 38 (4), 67–76. doi:10.3787/j.issn.1000-0976.2018.04.008
- Feng, Y., Xiao, X. M., Gao, P., Wang, E. Z., Hu, D. F., Liu, R. B., et al. (2023). Restoration of sedimentary environment and geochemical features of deep marine Longmaxi shale and its significance for shale gas: a case study of the Dingshan area in the Sichuan Basin, South China. *Mar. Pet. Geol.* 151, 106186. doi:10.1016/j.marpetgeo.2023.106186
- Furmann, A., Mastalerz, M., Schimmelmann, A., Pedersen, P. K., and Bish, D. (2014). Relationships between porosity, organic matter, and mineral matter in mature organic-rich marine mudstones of the Belle Fourche and Second White Specks formations in Alberta, Canada. *Mar. Pet. Geol.* 54, 65–81. doi:10.1016/j.marpetgeo.2014.02.020
- Gao, Z. Y., Fan, Y. P., Xuan, Q. X., and Zheng, G. W. (2020). A review of shale pore structure evolution characteristics with increasing thermal maturities. *Adv. Geo-Energy Res.* 4 (3), 247–259. doi:10.46690/ager.2020.03.03
- He, Q., Dong, T., He, S., and Zhai, G. Y. (2019). Methane adsorption capacity of marine-continental transitional facies shales: the case study of the Upper Permian Longtan Formation, northern Guizhou Province, Southwest China. *J. Petroleum Sci. Eng.* 183, 106406. doi:10.1016/j.petrol.2019.106406
- Hu, T., Wu, G. Y., Xu, Z., Pang, X. Q., Liu, Y., and Yu, S. (2022). Potential resources of conventional, tight, and shale oil and gas from Paleogene Wenchang Formation source rocks in the Huizhou Depression. *Adv. Geo-Energy Res.* 6 (5), 402–414. doi:10.46690/ager.2022.05.05
- Jin, Z. J. (2023). Hydrocarbon accumulation and resources evaluation: recent advances and current challenges. *Adv. Geo-Energy Res.* 8 (1), 1–4. doi:10.46690/ager.2023.04.01
- Lamberson, M. N., and Bustin, R. M. (1993). Coalbed methane characteristics of Gates Formation coals, northeastern British Columbia; effect of maceral composition. *AAPG Bull.* 77 (12), 2062–2076. doi:10.1306/bdff8fd8-1718-11d7-8645000102c1865d
- Li, J. R., Yang, Z., Wu, S. T., and Pan, S. Q. (2021). Key issues and development direction of petroleum geology research of source rock strata in China. *Adv. Geo-Energy Res.* 5 (2), 121–126. doi:10.46690/ager.2021.02.02
- Li, Y. J., Song, L. H., Tang, Y. J., Zuo, J. P., and Xue, D. J. (2022). Evaluating the mechanical properties of anisotropic shale containing bedding and natural fractures with discrete element modeling. *Int. J. Coal Sci. Technol.* 9 (1), 18. doi:10.1007/s40789-022-00473-5
- Liu, S. G., Deng, B., Sun, W., Song, J. M., Jiao, S., Ye, Y. H., et al. (2020). Sichuan Basin be a super petroliferous basin? *J. Xihua Univ. Nat. Sci. Ed.* 39 (5), 20–35. doi:10.12198/j.issn.1673-159X.3783
- Loucks, R. G., Reed, R. M., Ruppel, S. C., and Jarvie, D. M. (2009). Morphology, genesis, and distribution of nanometer-scale pores in siliceous mudstones of the Mississippian Barnett Shale. *J. Sediment. Res.* 79, 848–861. doi:10.2110/jsr.2009.092
- Lu, C. G., Xiao, X. M., Gai, H. F., Feng, Y., Li, G., Meng, G. M., et al. (2023). Nanopore structure characteristics and evolution of type III kerogen in marine-continental

Publisher's note

All claims expressed in this article are solely those of the authors and do not necessarily represent those of their affiliated organizations, or those of the publisher, the editors and the reviewers. Any product that may be evaluated in this article, or claim that may be made by its manufacturer, is not guaranteed or endorsed by the publisher.

transitional shales from the Qinshui basin, northern China. *Geoenergy Sci. Eng.* 221, 211413. doi:10.1016/j.geoen.2022.211413

Qiu, Z., Song, D. J., Zhang, L. F., Zhang, Q., Zhao, Q., Wang, Y. M., et al. (2021). The geochemical and pore characteristics of a typical marine–continental transitional gas shale: a case study of the Permian Shanxi Formation on the eastern margin of the Ordos Basin. *Energy Rep.* 7, 3726–3736. doi:10.1016/j.egyr.2021.06.056

Ross, D. J. K., and Bustin, R. M. (2008). Characterizing the shale gas resource potential of Devonian–Mississippian strata in the Western Canada Sedimentary Basin: application of an integrated formation evaluation. *AAPG Am. Assoc. Pet. Geol. Bull.* 92 (1), 87–125. doi:10.1306/09040707048

Sander, R., Pan, Z., Conell, L. D., Camilleri, M., Grigore, M., and Yang, Y. (2018). Controls on methane sorption capacity of Mesoproterozoic gas shales from the Beetaloo Sub-basin, Australia and global shales. *Int. J. Coal Geol.* 199, 65–90. doi:10.1016/j.coal.2018.09.018

Shi, X. W., Wu, W., Zhou, S. W., Tian, C., Li, D., Li, D. Y., et al. (2022). Adsorption characteristics and controlling factors of marine deep shale gas in southern Sichuan Basin, China. *J. Nat. Geoscience* 7, 61–72. doi:10.1016/j.jnggs.2022.04.001

Tang, S. H., and Fan, E. P. (2014). Methane adsorption characteristics of clay minerals in organic-rich shales. *J. China Coal Soc.* 39 (8), 1700–1706. doi:10.13225/j.cnki.jccs.2014.9015

Thommes, M., Kaneko, K., Neimark, A. V., Olivier, J. P., Rodriguez-Reinoso, F., Rouquerol, J., et al. (2015). Physisorption of gases, with special reference to the evaluation of surface area and pore size distribution (IUPAC Technical Report). *Pure Appl. Chem.* 87 (9–10), 1051–1069. doi:10.1515/pac-2014-1117

Wang, E. Z., Feng, Y., Guo, T. L., and Li, M. W. (2022a). Oil content and resource quality evaluation methods for lacustrine shale: a review and a novel three-dimensional quality evaluation model. *Earth-Sci. Rev.* 232, 104134. doi:10.1016/j.earscirev.2022.104134

Wang, E. Z., Feng, Y., Guo, T. L., Li, M. W., Xiong, L., Lash, G. G., et al. (2023a). Sedimentary differentiation triggered by the Toarcian Oceanic Anoxic Event and formation of lacustrine shale oil reservoirs: organic matter accumulation and pore system evolution of the Early Jurassic sedimentary succession, Sichuan Basin, China. *J. Asian, Earth. Sci.* 256, 105825. doi:10.1016/j.jseas.2023.105825

Wang, E. Z., Guo, T. L., Li, M. W., Li, C. R., Dong, X. X., Zhang, N. X., et al. (2022b). Exploration potential of different lithofacies of deep marine shale gas systems: insight into organic matter accumulation and pore formation mechanisms. *J. Nat. Gas. Sci. Eng.* 102, 104563. doi:10.1016/j.jngse.2022.104563

Wang, E. Z., Guo, T. L., Liu, B., Li, M. W., Xiong, L., Dong, X. X., et al. (2022c). Lithofacies and pore features of marine-continental transitional shale and gas enrichment conditions of favorable lithofacies: a case study of Permian Longtan Formation in the Lintanchang area, southeast of Sichuan Basin, SW China. *Pet. Explor. Dev.* 49 (6), 1310–1322. doi:10.1016/s1876-3804(23)60351-9

Wang, P. W., Nie, H. K., Liu, Z. B., Sun, C. X., Cao, Z., Wang, R. Y., et al. (2023b). Differences in pore type and pore structure between silurian Longmaxi marine shale and jurassic dongyuemiao lacustrine shale and their influence on shale-gas enrichment. *Minerals* 13, 190. doi:10.3390/min13020190

Wang, X. N., Li, J. R., Jiang, W. Q., Zhang, H., Feng, Y. L., and Yang, Z. (2022d). Characteristics, current exploration practices, and prospects of continental shale oil in China. *Adv. Geo-Energy Res.* 6 (6), 454–459. doi:10.46690/ager.2022.06.02

Wang, W. Y., Pang, X. Q., Chen, Z. X., Chen, D. X., Ma, X. H., Zhu, W. P., et al. (2020). Improved methods for determining effective sandstone reservoirs and evaluating hydrocarbon enrichment in petroliferous basins. *Appl. Energy* 261, 114457. doi:10.1016/j.apenergy.2019.114457

Wang, W. Y., Pang, X. Q., Wang, Y. P., Chen, Z. X., Li, C. R., Ma, X. H., et al. (2022e). Hydrocarbon expulsion model and resource potential evaluation of high-maturity marine source rocks in deep basins: example from the Ediacaran microbial dolomite in the Sichuan Basin, China. *Pet. Sci.* 19 (6), 2618–2630. doi:10.1016/j.petsci.2022.11.018

Wu, J., Wang, H. Y., Shi, Z. S., Wang, Q., Zhao, Q., Dong, D. Z., et al. (2021a). Favorable lithofacies types and genesis of marine-continental transitional black shale: a case study of Permian Shanxi Formation in the eastern margin of Ordos Basin, NW China. *Pet. Explor. Dev.* 48 (6), 1315–1328. doi:10.1016/s1876-3804(21)60289-6

- Wu, Z. Y., Zhao, X. Z., Wang, E. Z., Pu, X. G., Lash, G., Han, W. Z., et al. (2021b). Sedimentary environment and organic enrichment mechanisms of lacustrine shale: a case study of the paleogene shahejie formation, qikou sag, Bohai bay basin. *Palaeogeogr. Palaeoclimatol. Palaeoecol.* 573, 110404. doi:10.1016/j.palaeo.2021.110404
- Xin, D., Zhang, S. H., Tang, S. H., Xi, Z. D., and Jia, T. F. (2023). Influence of rock properties and prediction on the methane storage capacity in marine-continental transitional shale and coal from Northern China. *J. Asian, Earth. Sci.* 254, 105740. doi:10.1016/j.jseae.2023.105740
- Xu, J. Z., Wu, K. L., Li, R., Li, Z. D., Li, J., Xu, Q. L., et al. (2019). Nanoscale pore size distribution effects on gas production from fractal shale rocks. *Fractals* 27 (8), 1950142. doi:10.1142/s0218348x19501421
- Yang, C., Zhang, J. C., Han, S. B., Xue, B., and Zhao, Q. R. (2016). Classification and the developmental regularity of organic-associated pores (OAP) through a comparative study of marine, transitional, and terrestrial shales in China. *J. Nat. Gas. Sci. Eng.* 36, 358–368. doi:10.1016/j.jngse.2016.10.044
- Yang, J. Q., Zhang, J. T., He, Z. L., and Zhang, T. (2023). Paleoenvironment reconstruction of the middle ordovician thick carbonate from western Ordos Basin, China. *Pet. Sci.* 20 (1), 48–59. doi:10.1016/j.petsci.2022.08.027
- Yin, K. G., Zhang, C., Dan, C. A., Rao, D. Q., Li, Q. F., and Gao, Y. (2021). Geological characteristics and resource potential of the transitional shale gas in the Zhaotong national shale gas demonstration area. *Nat. Gas. Ind.* 41 (1), 30–35.
- Yin, S. L., Feng, K. Y., Nie, X., Chen, Q., Liu, Y., and Wang, P. L. (2022). Characterization of marine shale in Western Hubei Province based on unmanned aerial vehicle oblique photographic data. *Adv. Geo-Energy Res.* 6 (3), 252–263. doi:10.46690/ager.2022.03.08
- Zhang, P., Wang, Y., Zhang, X., Wei, Z., Wang, G., Zhang, T., et al. (2022). Carbon, oxygen and strontium isotopic and elemental characteristics of the Cambrian Longwangmiao Formation in South China: paleoenvironmental significance and implications for carbon isotope excursions. *Gondwana Res.* 106, 174–190. doi:10.1016/j.gr.2022.01.008
- Zhang, P. Y., Wang, Y. L., Wei, Z. F., Wang, G., Zhang, T., He, W., et al. (2023). Influence of the late Ordovician-early Silurian paleoenvironment and related geological processes on the organic matter accumulation and carbon isotope excursion. *Paleoceanogr. Paleoclimatology* 38, e2023PA004628. doi:10.1029/2023pa004628
- Zhou, S. W., Ning, Y., Wang, H. Y., Liu, H. L., and Xue, H. Q. (2018). Investigation of methane adsorption mechanism on Longmaxi shale by combining the micropore filling and monolayer coverage theories. *Adv. Geo-Energy Res.* 2 (3), 269–281. doi:10.26804/ager.2018.03.05
- Zhou, T. Q., Wu, C. D., Guan, X. T., Wang, J. L., and Jiao, Y. (2022). Coupling relationship between reservoir densification and hydrocarbon emplacement in the Jurassic Badaowan Formation sandstone reservoirs of the southern Junggar Basin, China. *Geol. J.* 57 (7), 2473–2496. doi:10.1002/gj.4429
- Zhou, T. Q., Zhu, Q. Z., Zhu, H. Y., Zhao, Q., Shi, Z. S., Zhao, S. X., et al. (2023). Relative Sea-level fluctuations during rhuddanian–aeronian transition and its implication for shale gas sweet spot forming: a case study of luzhou area in the southern Sichuan Basin, SW China. *J. Mar. Sci. Eng.* 11 (9), 1788. doi:10.3390/jmse11091788
- Zou, C. N., Dong, D. Z., Wang, Y. M., Li, X. J., Huang, J. L., Wang, S. F., et al. (2016). Shale gas in China: characteristics, challenges and prospects (II). *Pet. explor. Dev.* 43 (2), 182–196. doi:10.1016/s1876-3804(16)30022-2
- Zou, C. N., Zhao, Q., Cong, L. Z., Wang, H. Y., Shi, Z. S., Wu, J., et al. (2021). Development progress, potential and prospect of shale gas in China. *Nat. Gas. Ind.* 41 (1), 1–14. doi:10.3787/j.issn.1000-0976.2021.01.001